Spectral hole depth dependence on optical length in Tm^{3+}:YAG within cryogenic temperature range

Ma Xiurong[1,2], Wang Xiayang [1,2]

(1. Engineering Research Center on Communication Devices (Ministry of Education), School of Computer and Communication Engineering, Tianjin University of Technology, Tianjin 300384, China; 2. Tianjin Key Laboratory of Film Electronic and Communication Device, School of Electronic Information Engineering, Tianjin University of Technology, Tianjin 300384, China)

Abstract: Spectral hole depth dependence on optical length in Tm^{3+}:YAG was theoretically and experimentally investigated. A novel model was proposed to analyze the spectral hole depth dependence on optical length. With the proposed model, the spectral hole depth dependence on optical length had been derived theoretically. According to the theoretic result, when temperature was higher than 4 K, the maximum spectral hole depth could be found by choosing the optimum optical length. The theoretical analysis were experimentally tested using spectral hole burning in Tm^{3+}:YAG for a couple of configurations and sizes of the beams.

Key words: spectral hole depth; optical length; Tm^{3+}:YAG; temperature

CLC number: TP911.73 **Document code**: A **Article ID**: 1007-2276(2015)03-0964-05

低温条件下光学厚度对Tm^{3+}:YAG 材料光谱烧孔孔深的影响

马秀荣[1,2],王夏洋[1,2]

(1. 天津理工大学 计算机与通信工程学院 光电器件与通信技术教育部通信研究中心,天津 300384;
2. 天津理工大学 电子信息学院 天津理工大学薄膜电子与通信器件重点实验室,天津 300384)

摘 要:通过理论与实验研究了光学厚度对 Tm^{3+}:YAG 材料光谱烧孔孔深的影响。提出了一种用于分析光学厚度对光谱烧孔孔深影响的新模型。该模型从理论上推导了烧孔孔深与光学厚度的关系。根据提出的理论模型,当温度大于 4 K 时,通过选择合适的光学厚度可以使光谱烧孔孔深得到最大值。最后通过使用合适的激光与 Tm^{3+}:YAG 材料所形成的光谱烧孔实验证明了实验结果与理论分析是相一致的。

关键词:光谱烧孔孔深; 光学厚度; Tm^{3+}:YAG; 温度

收稿日期:2014-07-11; **修订日期**:2014-08-16

基金项目:天津市科技创新专项基金(10FDZDGX00400)

作者简介:马秀荣(1961-),女,博士生导师,博士,主要从事光通信及移动通信方面的研究。Email:maxiurong@gmail.com

0 Introduction

Spectral-hole-burning (SHB) techniques in rare-earth-doped crystals have been proposed and demonstrated, providing instantaneous high-bandwidth over 10 GHz, correlation time lengths of several microseconds, and large dynamic range [1]. Applications, include RF signal processing[2], optical storage[3], slow light research[4-5], and laser frequency stabilization[6]. In RF signal processing, the spectral hole depth [7] and width [8] are two most important parameters which limits signal-to-noise, sensitivity, dynamic range, and resolution. These parameters are sensitive to optical length and temperature. A model is proposed to investigate temperature dependence of spectral hole depth [9]. However, the theoretical model on optical length dependence of spectral hole depth has not been reported yet.

In this paper, the spectral hole depth dependence on optical length in Tm^{3+}:YAG crystal within cryogenic temperature range is discussed in detail. First, the absorption coefficient dependence on temperature and optical length is discussed, then the spectral hole dependence on optical length within cryogenic temperature range is studied. The proposed model is used to deduce that at same temperature, the readout spectral hole depth increases to maximum and then decreases with the increasing optical length, at the same optical length, readout spectral hole depth decreases as temperature increasing and almost keeps a constant below a temperature. The experimental demonstration is performed in Tm^{3+}:YAG within cryogenic temperature range. Numerical simulations keep consistent with experimental results. According to the theoretical result, by selecting the suitable optical length, the maximum hole depth can be found, when temperature is above 4 K.

1 Model of spectral hole depth optical length dependence

Spectral hole burning is the process by which spectrally varying absorption features are formed in materials. Tm^{3+}:YAG can be treated as a two level system[10]. Illuminating SHB crystals at frequencies in the inhomogeneous band induces transitions from the ground state to the excited state for resonant ions, leaving spectral holes in the absorption band at the resonant frequencies[11].

In inhomogeneous broadening media, for a weak beam, the small-signal absorption coefficient α_0 can be written as [2]

$$\alpha_0=-\int_{-\infty}^{\infty} N\sigma G(f)l(f-f_0)\mathrm{d}f \tag{1}$$

Where N is the absorber number density, σ is the absorption cross section.

Inhomogeneous and homogeneous broadening both contribute to the effective absorption. It assumes that the absorbers are distributed along a Gaussian inhomogeneous line[3]:

$$G(f)=\frac{T_2^*}{\sqrt{\pi}}\exp[-(fT_2^*)^2] \tag{2}$$

Where $1/T_2^*$ is the inhomogeneous linewidth.

At room temperature, phonons interact with the ions, homogeneously broadening the ionic line width. Cooling the crystal to liquid helium temperature suppresses phonon broadening, sharpening each ion′s linewidth to the limit given by a Lorentzian of width $1/T_2$[12],

$$\ell(f-f_0)=\frac{(1/T_2)^2}{(1/T_2)^2+(f-f_0)^2} \tag{3}$$

This affects the probability of an ion resonant at f_0 absorbing an incident photon.

The optical coherence time T_2 can be expressed as[7]

$$T_2=T_1\exp(\hbar\omega/(k_BT)) \tag{4}$$

Where T_1 is the excited-state lifetime, T is the temperature, $\hbar\omega$ is the phonon energy, and k_B is the

Boltzmann constant.

Substitute Eq. (4) and Eq. (3) into Eq. (1), which gives

$$\alpha_0=-\int_{-\infty}^{\infty} N\sigma G(f)\frac{1}{1+[T_1\exp(\hbar\omega/(k_BT))(f-f_0)]^2}\mathrm{d}f \quad (5)$$

From Eq. (5) it is seen that the small-signal absorption coefficient α_0 dependence on temperature T as shown in Fig.1.

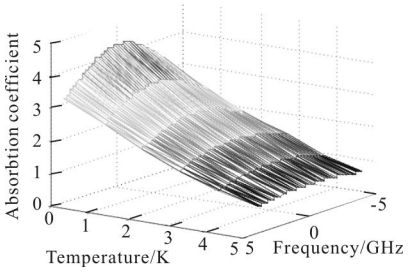

Fig.1 Absorption coefficient dependence on temperature for a weak beam

From Fig.1, it is known that the absorption coefficient decreases as the temperature increasing.

In the above the relationship between temperature and absorption coefficient is discussed in the case of a weak beam addresses the crystal.

As the beam intensity increases, however, the absorption at the beam frequency decreases. The population inversion $w(z, f_0)$ affects the absorption coefficient, and then the absorption coefficient can be rewrited as below[9]:

$$\alpha_1(z)=\int_{-\infty}^{\infty} N\sigma G(f)\ell(f-f_0)w(z,f_0)\mathrm{d}f \quad (6)$$

At steady state, the population inversion is given by[11],

$$w(z,f_0)=\frac{w_{eq}}{1+[I(z)/I_{sat}]\ell(f-f_0)} \quad (7)$$

When the signal beam intensity equals the saturation intensity, the inversion falls to half of its equilibrium value, hence the term saturation intensity. For large values of I_s, the inversion asymptotically approaches 0, indicating that the medium becomes transparent at the signal frequency for high signal intensities. As no external fields are present and all the absorbers are initially in the ground state, the equilibrium inversion is $w_{eq}=-1$.

By introducing the saturation intensity as[10]:

$$I_{sat}=\frac{c\varepsilon}{2}\left|\frac{\hbar}{\mu_{12}}\right|^2\frac{1}{T_1T_2} \quad (8)$$

Where ε is the material permittivity, μ_{12} is the electric dipole moment.

Then the absorption coefficient can be writen, which is illuminated by the signal beam as:

$$\alpha_1(z)=-\int_{-\infty}^{\infty}\frac{N\sigma G(f)\ell(f-f_0)}{1+[I(z)/I_{sat}]\ell(f-f_0)}\mathrm{d}f \quad (9)$$

Figure 2 shows the absorption coefficient at the beam frequency.

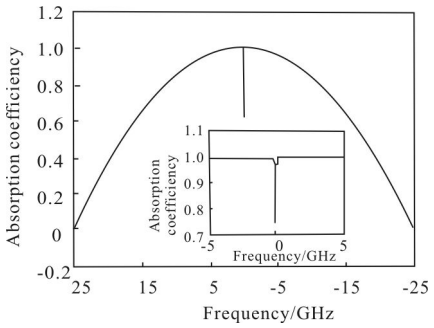

Fig.2 Change of the absorption coefficient at the beam frequency

From Fig.2, it can be seen that with the beam intensity increasing, the absorption coefficient changed at the beam frequency, and the change in absorption at the beam frequency is the spectral hole.

According to Beer′s Law, the intensity of the incident field evolves is known as[12],

$$\frac{\mathrm{d}I(z)}{\mathrm{d}z}=-2\alpha_0I(z) \quad (10)$$

By solving this differential equation, it can be gotten:

$$I(z)=2I_0\exp\int_0^L-\alpha_0\mathrm{d}z \quad (11)$$

Where L is the crystal thickness.

A differential detector senses the read and background beams, producing a differential current[8]:

$$i_d(L,T,f,f_s)=i_s(L,T,f,f_s)-i_b(L,T,f,f_s)= \quad (12)$$
$$2RI_0\left\{\exp\left[\int_0^L-\alpha_1(z)\mathrm{d}z\right]-\exp[-\alpha_0L]\right\}$$

Where i_s and i_b are the photocurrents produced by the read and background beams respectively, and R is the detector responsivity in A/W. $f_s=f_0$ is the read beam

oscillating frequency.

From Eq. (12), the relationship among optical length, temperature and the spectral hole depth can be obtained.

The readout spectral hole depth dependent on optical length and temperature is simulated by Eq. (12), as shown in Fig.3.

Figure 3 shows that the spectral hole depth is determined by optical length and temperature.

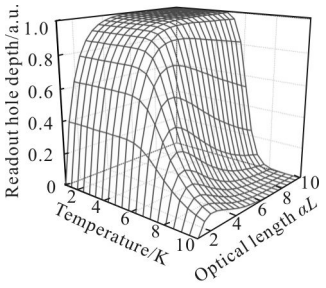

Fig.3 Temperature dependence on readout spectral hole depth with different optical length

According to the simulation results, when temperature is fixed, the spectral hole depth varies with the optical length, as shown in Fig.4.

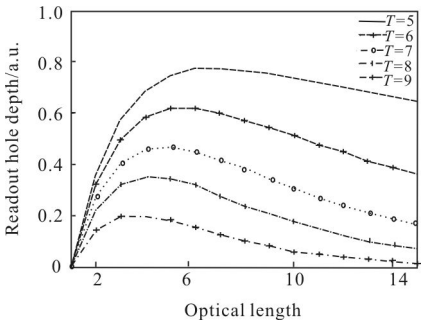

Fig.4 Readout spectral hole depth dependence on optical length

From Fig.4, it can be seen that the readout spectral hole depth increases to maximum and then decreases with the increasing optical length.

Figure 5 shows that the spectral hole depth is mainly determined by optical length when the temperature is below 4 K, and the temperature is the dominant effect on the hole depth when it is higher than 4 K. Consequently, an optimum optical length can be selected to get the maximum hole depth when temperature higher than 4 K.

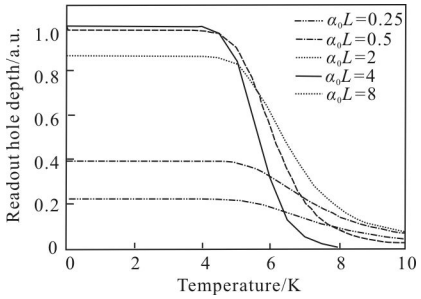

Fig.5 Temperature dependence on readout spectral hole depth with different optical lengths

3 Experimental demonstration

The experimental setup for spectral hole analysis in Tm^{3+}:YAG is shown in Fig.6. The key element is the SHB material which is a 2.5 mm–long 0.5–at.%–doped Tm^{3+}:YAG crystal which is placed in a cryostat (OXFORD PT403, CP8300). Since the limit of the experimental conditions, one crystal is used in the experiment. The temperature is changed from 4 K to 11.2 K (limited by cryogenic equipment) with the interval of 0.5 K by using liquid helium. A stabilized external cavity diode laser (New Focus 6700) produces the laser to burn a hole at the write laser frequency into the crystal inhomogeneous profile[12]. The laser source intensity is fixed at emitting at a vacuum wavelength centered at 793 nm. A trigger signal produced by AWG (Agilent 33250A) is controlling the frequency–chirped read beam from the read source with weak intensity. The chirp band is 1 GHz wide and chirp rate is set to k=0.1MHz/s. The two read beams are combined at the differential detector. The digitizing oscilloscope (Agilent 54833D MSO) records spectral hole.

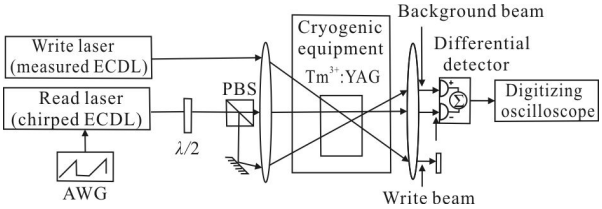

AWG: arbitrary waveform generator; PBS: polarizing beam splitters; ECDL: external cavity diode laser

Fig.6 Experimental setup

Figure 7 shows that the theoretical result is in good agreement with experimental result. The hole depth keeps invariable once temperature below about 4 K when $\alpha_0 L$ =2, and decreases with the temperature increasing approximately by an exponential way.

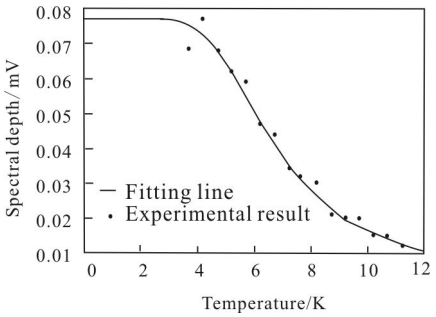

Fig.7 Spectral hole depth dependent on temperature

4 Conclusion

In summary, a model is proposed to achieve spectral hole in rare earth doped YAG crystal dependence on optical length within cryogenic temperature range. This model is established according to the absorption coefficient derived from optical Bloch equations, and the temperature dependence on spectral hole. From the theoretic curve, the maximum hole depth can be found at a given temperature by choosing the optical length. However, from the proposed model, one optical thickness at 2.5 mm is only choosen and it will changing different optical thickness in the future experiment.

References:

[1] Cole Z, Bottger T, Mohan R K, et al. Coherent integration of 0.5 GHz spectral holograms at 1536 nm using dynamic biphase codes [J]. ***Applied Physics Letters***, 2002, 81(19): 3525-3527.

[2] Gorju G, Crozatier V, Lorgeré I, et al. 10-GHz bandwidth RF spectral analyzer with MHz resolution based on spectral hole burning in Tm^{3+}:YAG[J]. ***IEEE Photonics Technology Letters***, 2005, 17(11): 2385-2387.

[3] Schlottau F, Colice M, Wagner K H, et al. Spectral hole burning for wideband, high-resolution radio-frequency spectrum analysis [J]. ***Optics Letters***, 2005, 30(22): 3003-3005.

[4] Song Minqing, Hou Shanglin, Zhang Baoxia, et al. Investigation on slow light of photonic crystal fiber Bragg gratings [J]. ***Infrared and Laser Engineering***, 2013, 42 (6): 1547-1552. (in Chinese)
宋民青, 侯尚林, 张保侠, 等. 光子晶体光纤布拉格光栅慢光的研究[J]. 红外与激光工程, 2013, 42(6): 1547-1552.

[5] Lu Hui, Zhang Lijun, Zheng Zhanqi, et al. Time-delay and phase-delay methods for slow light measurement in photonic crystal waveguide[J]. ***Infrared and Laser Engineering***, 2012, 41(2): 347-352. (in Chinese)
鲁辉, 张立军, 郑占旗, 等. 用于光子晶体波导慢光测试的时间和相位延迟方法 [J]. 红外与激光工程, 2012, 41(2): 347-352.

[6] Qu Ronghui, Cai Haiwen. Narrow linewidth lasers with high stability [J]. ***Infrared and Laser Engineering***, 2009, 38 (6): 1033-1038. (in Chinese)
瞿荣辉, 蔡海文. 高稳定度窄线宽激光器的研究[J]. 红外与激光工程, 2009, 38(6): 1033-1038.

[7] Colice M, Schlottau F, Wagner K H. Broadband radio-frequency spectrum analysis in spectral-hole-burning media [J]. ***Applied Optics***, 2006, 45(25): 6393-6408.

[8] Ivan Lorgeré, Loïc Menagér, Vinvent Lavielle, et al. Demonstration of a radio-frequency spectrum analyzer based on spectral hole burning[J]. ***Journal of Modern Optics***, 2002, 49: 2459-2475.

[9] Lei C, Ma Xiurong, Wei W, et al. Characterization of spectral hole depth in Tm^{3+}:YAG within the cryogenic temperature range [J]. ***Chinese Physics B***, 2013, 22(6): 064213.

[10] Colice M, Schlottau F, Wagner K, et al. RF spectrum analysis in spectral hole burning media [C]// Optical Science and Technology, the SPIE 49th Annual Meeting, International Society for Optics and Photonics, 2004: 132-139.

[11] Schlottau F, Colice M, Wagner K H, et al. Spectral hole burning for wideband, high-resolution radio-frequency spectrum analysis[J]. ***Optics Letters***, 2005, 30(22): 3003-3005.

[12] Chang T, Tian M, Mohan R K, et al. Recovery of spectral features readout with frequency-chirped laser fields[J]. ***Optics Letters***, 2005, 30(10): 1129-1131.